Dynamic Fluorescence Probing of the Local Environments within Amphiphilic Starlike Macromolecules

Lotti Frauchiger, Hideaki Shirota,† Kathryn E. Uhrich,* and Edward W. Castner, Jr.*

Department of Chemistry and Chemical Biology, Rutgers University, 610 Taylor Road, Piscataway, New Jersey 08854-8087

Received: March 19, 2002

Steady-state and time-resolved fluorescence spectroscopies were used to investigate the local environments of coumarin 102 (C102) probe molecules when encapsulated within an amphiphilic starlike macromolecule (ASM). ASMs are promising surfactant-type nanoscale transporters of hydrophobic drug molecules. They consist of a hydrophobic core, in which small, hydrophobic molecules such as C102 can be encapsulated, and a hydrophilic shell that makes the whole assembly water-soluble. Steady-state fluorescence spectroscopy revealed that C102 molecules sense a very polar environment when encapsulated in ASMs. Both time-correlated single-photon counting and fluorescence upconversion techniques indicated that the solvent reorganization and diffusive reorientation of the C102 solvatochromic fluorescent probe are significantly slowed compared to the rates in aqueous solutions. These results provide insight into the dynamics of drugs encapsulated within ASMs.

Introduction

Amphiphilic starlike macromolecules (ASMs) are a class of polymeric surfactants that have recently emerged as promising nanoscale drug carriers.[1,2] The design concept is that the inner hydrophobic core of the ASM solubilizes lipophilic molecules (e.g., drugs) and the outer hydrophilic shell makes the entire assembly water soluble. ASMs are micelle-like constructs in which the surfactant chains are covalently bound together rather than loosely aggregated. ASMs have an advantage over conventional micelles because they are thermodynamically stable over a broad range of physical and chemical conditions. In contrast, conventional polymeric micelles such as amphiphilic block copolymers are thermodynamically unstable with respect to extremes of concentration, pH, and temperature.[3−5] Torchilin recently reviewed polymeric micelles.[6] The ASM used for this study (see Scheme 1) consists of a trisphenolic unit (black), sugar units (mucic acid, green), fatty acids (hexanoic acid, red), and poly(ethylene glycol) (PEG) with a molecular weight of 5000 g mol^{-1} (blue). In addition to being highly water-soluble, these ASMs are noncytotoxic[7] and biodegradable,[8] characteristics that make them promising candidates for drug delivery applications.

Amphiphilic structures such as micelles are useful because they can water-solubilize hydrophobic molecules that would otherwise partition from water-based body fluids. Previous in vitro studies demonstrated that ASMs control the rate of drug diffusion but only when the drugs are encapsulated within the ASM structure.[2] Though the solubilization properties of polymeric surfactants have been widely studied,[4,9] little is known about the local environments sensed by the drug molecules when encapsulated in such core-shell structures. By defining dynamical fluctuations in the polymer−solvent environment within ASMs, we garner useful information on the mechanism of drug binding and release.

SCHEME 1: Chemical Structures of the Amphiphilic Starlike Macromolecule (ASM, $n = 110$) and Coumarin 102 (C102)

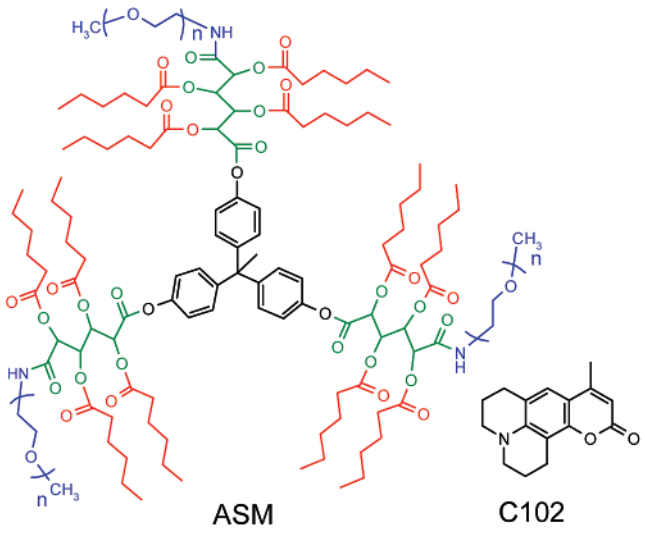

The studies reported herein describe the behavior of a hydrophobic molecule encapsulated within ASMs. Specifically, we report our investigation of the local environments within ASMs using time-dependent fluorescence Stokes shift (TDFSS) and fluorescence polarization anisotropy measurements. The rigid, solvatochromic molecule coumarin 102 (C102, see Scheme 1) was used as the fluorescence probe in this study.[10−12] Use of C102 as a solvation probe has been previously reported.[10,11,13] In addition to its suitable spectral properties, C102 has an octanol−water partition coefficient (log *P*) of 4.09 that is similar to that of many commonly used lipophilic drugs such as progesterone (log $P = 3.87$) and propoxyphone (log $P = 4.18$).[14]

* Corresponding authors. E-mail: uhrich@rutchem.rutgers.edu and castner@rutchem.rutgers.edu.

† Present Address: Department of General System Sciences, Graduate School of Arts and Sciences, University of Tokyo, 3-8-1 Komaba, Meguro-ku, Tokyo 153-8902, Japan.

10.1021/jp020746e CCC: $22.00
Published on Web 07/02/2002

Experimental Section

Materials. Laser-grade C102 (Kodak), HPLC-grade water (Acros), methoxypoly(ethylene glycol)amine (M_w = 5000 g mol^{-1}, Shearwater, PEG), and all the other chemicals (Sigma-Aldrich) were used as received. Spectrophotometric or HPLC-grade solvents were used for the steady-state absorption and emission measurements. ASMs were prepared as described by Liu et al.[1]

Methods. A procedure described by Hagan et al.[15] was used for the encapsulation of C102 into ASMs. The control solutions were prepared by dissolving C102 or C102 and PEG in water with 0.6 v/v% dimethylformamide (DMF), respectively.

Steady-state emission spectra were measured with an AVIV ratio spectrofluorometer (model ATF105) at a C102 concentration of 1×10^{-5} M. Cyclohexane, ethyl acetate, octanol, and water solvents were used to cover a wide range of polarity. An aqueous solution of C102 encapsulated in ASMs was also measured. The solutions were filtered through a 0.45-μm polytetrafluoroethylene (PTFE) filter (Whatman, Clifton, NJ) before use. The optical path length of the sample was 10 mm.

The time-correlated single-photon counting (TCSPC) studies were performed with a polymer concentration of 2×10^{-4} M (ASM and PEG) and a C102 concentration of 2×10^{-5} M. The polymer concentration for the fluorescence upconversion experiments was 2×10^{-4} M, with the corresponding C102 concentration ranging from 3×10^{-5} to 1×10^{-4} M. Thus, each ASM was loaded with zero or one C102 probe molecule.

The TCSPC and fluorescence upconversion instruments have been described elsewhere[16−18] but are outlined below. For the fluorescence upconversion instrument, second-harmonic light at 387 nm with an average power of 120 mW was obtained by using the fundamental light of a femtosecond titanium/sapphire laser (Spectra Physics Tsunami) at 773 nm with an average power of about 740 mW. The second-harmonic light was used to excite the sample. The remaining fundamental light was used as the gating beam to upconvert the fluorescence from the sample by phase-matched sum frequency generation in a 1.0-mm path length BBO crystal. The measured cross correlation between the second harmonic and fundamental had a full width at half-maximum of 220 fs. The angle between the polarization of the pump and gate beams was adjusted with a half-wave retarder to the magic angle (54.7°) for the solvation studies and to 0° or 90° for the fluorescence anisotropy studies. After passing through a spectrometer, the upconverted signal was detected with a photon counting system. The optical path length of the sample was 2 mm. The sample solutions were circulated during all measurements and were measured at room temperature (about 294 K). The solutions were filtered through a 0.45-μm PTFE filter (Whatman, Clifton, NJ) before use.

Results and Discussion

Figure 1 shows the steady-state emission spectra of C102 in a series of solutions of varying polarity. The C102 emission maximum varied from 408 to 490 nm as the solvent polarity was increased (from cyclohexane to water). An aqueous solution of ASMs with encapsulated C102 has an emission maximum of 487 nm, indicating that on average C102 was located in a very polar, water-like environment when encapsulated. The position of the emission maximum of C102 encapsulated in ASM is closer to that of water than to that of micelle solutions[19] or reverse micelle solutions.[20] The emission maximum for C102

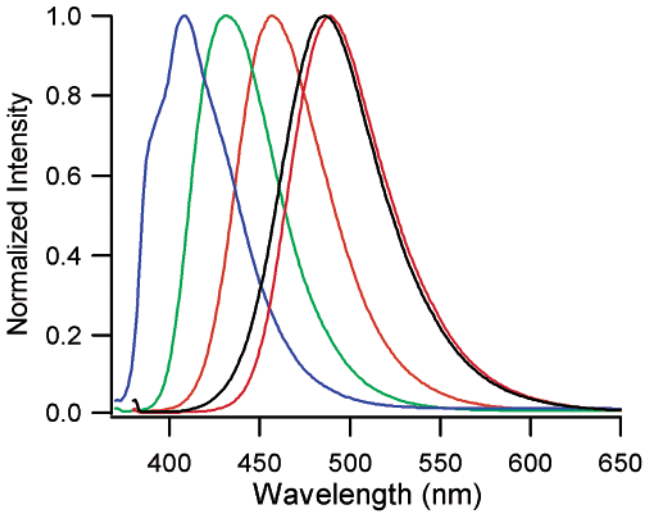

Figure 1. Steady-state emission spectra of C102 in a series of solutions of increasing polarity. From left to right (nonpolar to polar), the curves represent C102 in cyclohexane ($\epsilon_{20\ °C}$ = 2.0, blue), ethyl acetate ($\epsilon_{25\ °C}$ = 6.0, green), octanol ($\epsilon_{20\ °C}$ = 10.3, orange), ASM/water (black), and water ($\epsilon_{20\ °C}$ = 80.4, red).

in aqueous PEG (M_w = 4600 g mol^{-1}) solutions ranges from 462 nm (for neat PEG 400) to 490 nm for aqueous C102. For M_w = 4600 g mol^{-1} PEG, the emission varies from 470 to 485 nm for concentrations from 10 to 50 wt %. Note that the ASMs are intended to release the bound drug gradually over a period of several days, so a certain fraction of C102 is expected to be found in the bulk water solution outside the ASM. The disparity between the steady-state emission data and encapsulation[1] results was further investigated by means of two time-resolved emission methods: time-correlated single-photon counting (TCSPC) and fluorescence upconversion.

Figure 2 (top) shows the TCSPC transients in the wavelength range from 420 to 540 nm for C102 in aqueous ASM solutions over a 16-ns time window. Figure 2 (bottom) shows fluorescence upconversion transients from 445 to 540 nm for a 5-ps time window. The time dependence of the fluorescence transients for C102 encapsulated in ASMs results from the C102 dynamic solvatochromism or TDFSS. In solutions of ASMs with encapsulated C102, complex spectral dynamics were observed on subpicosecond time scales, as previously noted for aqueous solutions of coumarin dyes.[10,12,21−23] On the shortest time scales, the C102 emission dynamics differ only slightly from those of the aqueous C102 control solution: a rapid decay at the blue wavelengths (436−463 nm) occurs on a subpicosecond time scale for C102 in all aqueous solutions in the presence and absence of ASMs, after which a much longer time scale decay occurs. Similarly, the spectral region at the red edge (500−540 nm) shows the subpicosecond rise, with a subsequent nanosecond time scale rise in the C102/ASM solutions.

TDFSS dynamics are obtained from the energy relaxation of the excited-state solvatochromic probe. The solvation time correlation function is given by

$$S_\nu(t) = \frac{\bar{\nu}(t) - \bar{\nu}(\infty)}{\bar{\nu}(0) - \bar{\nu}(\infty)} \qquad (1)$$

The spectral reconstruction method[24,25] was used to obtain the time-dependent shift of the emission maximum of C102 in the aqueous ASM solutions. Because the time constants span three orders of magnitude, data from two methods (TCSPC and fluorescence upconversion) were considered. A Fortran program,

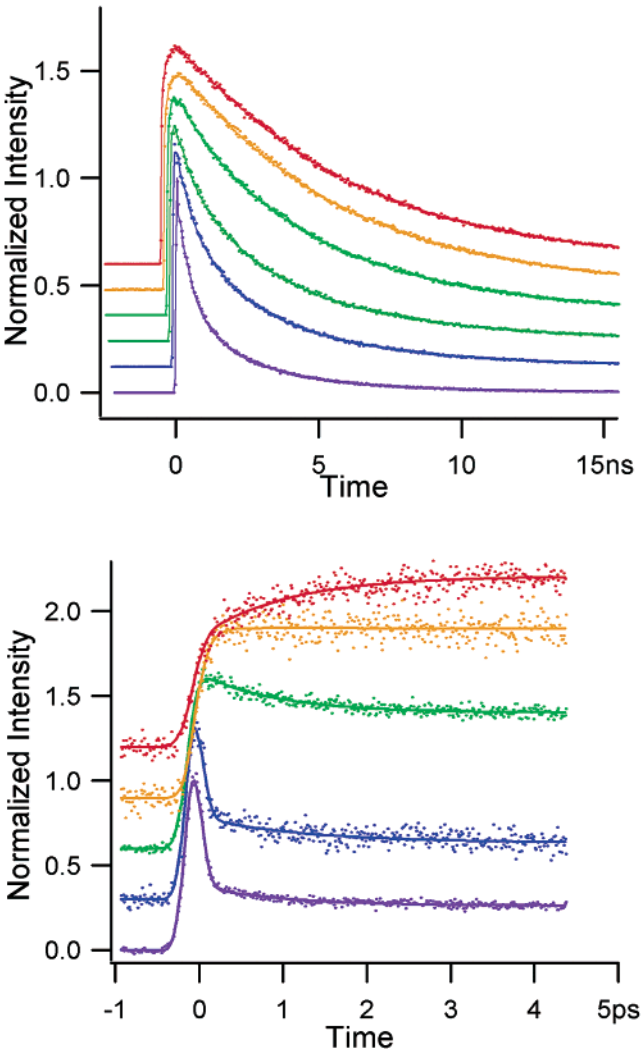

Figure 2. Top: Selected fluorescence transients for C102 in aqueous ASM solutions from 420−540 nm (TCSPC data) from bottom to top: 420, 436, 445, 463, 493, and 540 nm. Bottom: Selected fluorescence transients for C102 in aqueous ASM solutions from 445−540 nm (fluorescence upconversion data) from bottom to top: 445, 454, 463, 493, and 540 nm. The dots represent the data, and the solid lines show the nonlinear least-squares fits to multiexponential functions. Signals are offset to clarify the difference.

stshany2, that was obtained from Professor M. Maroncelli (Pennsylvania State University) was used to analyze the time-dependent fluorescence Stokes shifts.[25] The emission maximum time correlation function $S_\nu(t)$ for the aqueous C102/ASM solutions is best fit using a triexponential response. The solvation times (τ_i) and relative amplitudes (α_i) of C102 in ASM/water, PEG/water, and water were obtained by fitting the time-resolved first-moment frequencies with a single or biexponential function. These values are listed in Table 1. The shortest solvation time constant was obtained using a single-exponential fit to the time correlation function $S_\nu(t)$ constructed from the fluorescence upconversion data. The two longer exponential time constants were determined from the time correlation function $S_\nu(t)$ constructed from the TCSPC data.

As with previous TDFSS measurements of solvation dynamics obtained via the upconversion method, the time resolution obtained with the 200-fs full width at half-maximum (fwhm) upconversion instrument response precludes full resolution of the fastest component of the solvation dynamics. Only the more rapid dynamics, characterized by the average solvation time constant of <1 ps, were observed for the aqueous C102 and

TABLE 1: Solvation Time Constants (τ_i) and Normalized Amplitudes (α_i) of C102 in ASM/Water, PEG/Water, and Water Control Solutions

C102 solution	α_1	τ_1 (ps)	α_2	τ_2 (ps)	α_3	τ_3 (ps)
ASM/water	0.44[a]	0.95[b]	0.19[a]	361[a]	0.37[a]	3962[a]
PEG/water	1[b]	0.87[b]				
water	1[b]	0.95[b]				

[a] From TCSPC; time spacing: 36.4 ps/point. [b] From fluorescence upconversion; time spacing: 13 fs/point.

aqueous C102/PEG control solutions. This shortest average lifetime of <1 ps for the C102 Stokes shift in the ASM solutions is assigned to solvation in bulk water or a bulk-water-like environment and is similar to lifetimes observed for the coumarin 343 (C343) anion,[21] neutral C343,[22] and C102.[12] As in these prior studies, the limited time resolution precludes detection of the full spectrum of underdamped rotational and translational motions known to occur in liquid water.[26] The two larger time constants indicate that the reorganization process within the ASM was much slower than in neat nonaqueous solvents, for which the time constants for solvation dynamics range from 1 to 50 ps.[25] Similar observations were made for micelles,[19] reverse micelles,[27] emulsions,[23,28] and proteins.[29,30] These unusual fluorescence dynamics indicate that C102 in ASM solutions exhibits a solvation response with time constants that vary by more than three orders of magnitude.

The normalized reconstructed fluorescence spectra for C102 in ASM/water are shown in Figure 3. The time-dependent spectra were calculated from the fluorescence upconversion data for the time window of 0.01−5 ps after excitation and from the TCSPC data for the time window of 10 ps to 50 ns. Note that the spectrum narrows considerably for the longer time part of the TDFSS beyond 10 ps.

Figure 4 shows the complex time dependence of the average emission frequency. The data were obtained from fluorescence upconversion data for the short time window (0.2−10 ps) and from TCSPC for the longer time window (0.01−10 ns). For times <200 fs, vibronic relaxation led to a complex spectral evolution of the C102 emission involving two vibronic states, as has been reported for coumarin 153.[31]

Figure 5 shows the TCSPC fluorescence anisotropy decay $r(t)$ for the aqueous ASM solution with encapsulated C102, where $r(t)$ is defined as

$$r(t) = \frac{I_{||}(t) - I_{\perp}(t)}{I_{||}(t) + 2I_{\perp}(t)} \qquad (2)$$

and $I_{||}$ and $I_{\perp}$ are the fluorescence transients polarized parallel and perpendicular, respectively, to the polarization of the 387-nm excitation pulse.

The best fit to the anisotropy decay was obtained by using a triexponential function for the C102/ASM sample:

$$r(t) = a_{r1}\exp\left(\frac{-t}{\tau_{r1}}\right) + a_{r2}\exp\left(\frac{-t}{\tau_{r2}}\right) + a_{r3}\exp\left(\frac{-t}{\tau_{r3}}\right) \qquad (3)$$

The fluorescence anisotropies of C102 in the control samples (PEG/water and water) were measured using the upconversion technique, and they fit well to a single exponential function. The orientational relaxation time constants (τ_{ri}) and relative amplitudes (α_{ri}) of the fluorescence anisotropy decay of C102 in ASM/water, PEG/water, and water are provided in Table 2.

The longer time constants for the polarization anisotropy of 400 and 4100 ps provide additional evidence for C102 being

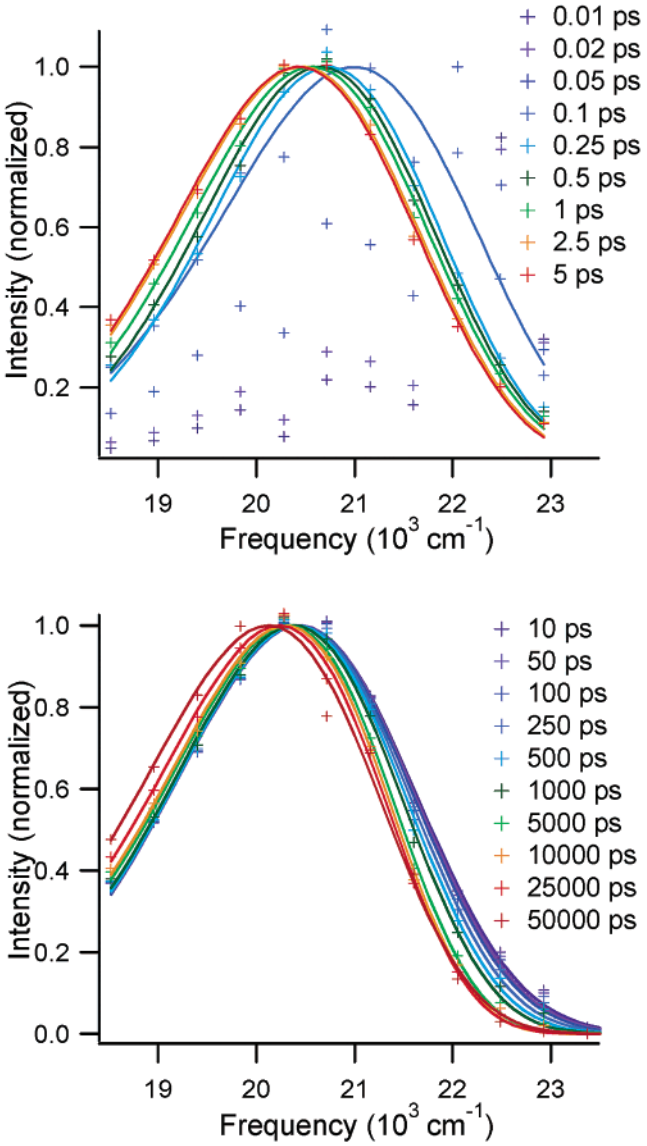

Figure 3. Normalized reconstructed fluorescence spectra for C102 in ASM/water. Top: Spectra were calculated from the fluorescence upconversion data. The times shown here are 0.01−5 ps after excitation in order of decreasing peak frequency. Bottom: Spectra were calculated from the TCSPC data. The times shown here are 10−50 000 ps.

encapsulated within the ASM but not rigidly bound. The results suggest that C102 in the ASM solution senses several heterogeneous local environments. A hydrodynamic interpretation of the 400- and 4100-ps time constants for the fluorescence anisotropy implies that C102 molecules within the ASMs experience frictional forces that are about 6 and 60 times greater, respectively, than those in water alone. Our results further suggest that the C102 molecules are not tightly bound within the ASM but rather that their movements are significantly slowed or restricted by the high local friction. The increased local friction probed by the C102 likely results from an increased microviscosity caused by the high density of fatty acid chains in the core and PEG chains in the shell.

Disordered and amorphous systems such as polymer solutions and glasses often display complex dynamical behaviors that are best described by a range or distribution of relaxation times,[32−34] whereas dynamics for more homogeneous chemical and physical phenomena may be described by discrete time constants.[21,25] When a distribution of rates description applies to such physical processes, the observed dynamics can often be fit by the

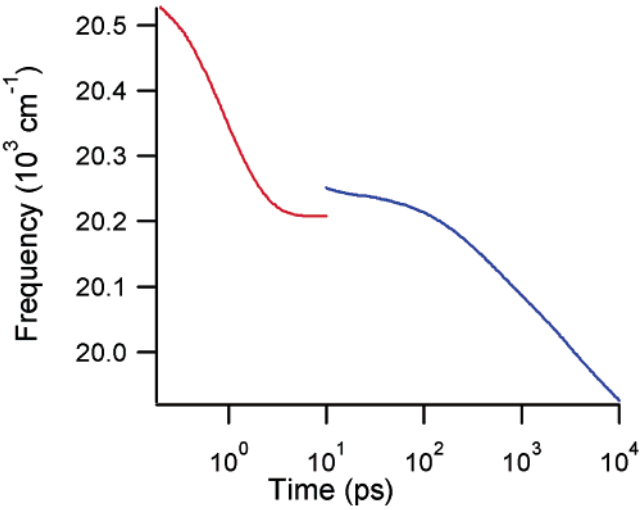

Figure 4. Evolution of the first-moment fluorescence frequency with time. The time window from 0.2 to 10 ps was calculated from fluorescence upconversion data, and the time window from 10 to 10 000 ps, from TCSPC data.

Kohlrausch, or stretched exponential, function

$$I(t) = \exp\left[-\left(\frac{t}{\tau_0}\right)^{\beta}\right] \qquad \text{where } 0 < \beta \leq 1 \tag{4}$$

For values of $\beta < 1$, the Kohlrausch function presents a decay that is steeper than that of the corresponding exponential ($\beta = 1$) function, and for longer times, a decay with a much flatter slope than that of the exponential. This trend is made more dramatic with the decreasing value of exponent β.

Dynamics in polymer solutions have previously been shown to exhibit stretched exponential character.[35−38] Our preliminary results from TDFSS and fluorescence anisotropy experiments on concentrated aqueous PEG solutions (10−50 wt % PEG) with M_w in the range of 200−20 000 also show this behavior.[39] The single-wavelength method[40,41] developed by Nagarajan et al. was applied to the study of C102 solvation dynamics in aqueous PEG because of the large number of samples with similar chemical properties. In brief, the emission of C102 at 420 nm was used to estimate the dynamical solvation correlation function $S_v(t)$ (see eq 1). In general, the observed transients can be fit reasonably well by a sum of two to five exponential functions. However, better fits are obtained using a simpler model function, the "single exponential plus Kohlrausch" function

$$I(\lambda = 420 \text{ nm}, t) = a_{\text{fl}} \exp\left(-\frac{t}{\tau_{\text{fl}}}\right) + a_{\text{solv}} \exp\left[-\left(\frac{t}{\tau_{\text{solv}}}\right)^{\beta}\right] \qquad \text{where } 0 < \beta \leq 1 \tag{5}$$

where τ_{fl} is the fluorescence lifetime measured at 480 nm and τ_{solv} is the frequency characterizing the broad distribution of dynamical solvation time constants.

For concentrated solutions of aqueous PEG with $M_w = 4600$ g mol^{-1} (10−50 wt %), the complex TDFSS dynamics are best described by the stretched exponential solvation model, though a sum of two exponentials works nearly as well.[39] However, the overall trend from $M_w = 200$−20 000 g mol^{-1} shows that the equivalent quality of fits for biexponential versus eq 5 for aqueous PEG ($M_w = 4600$ g mol^{-1}) is coincidental; the entire range can be best fit by the latter model, but only seldom does the biexponential model fit. The degree of nonexponentiality is severe, with values for β in eq 5 ranging from 0.2 to 0.7 for

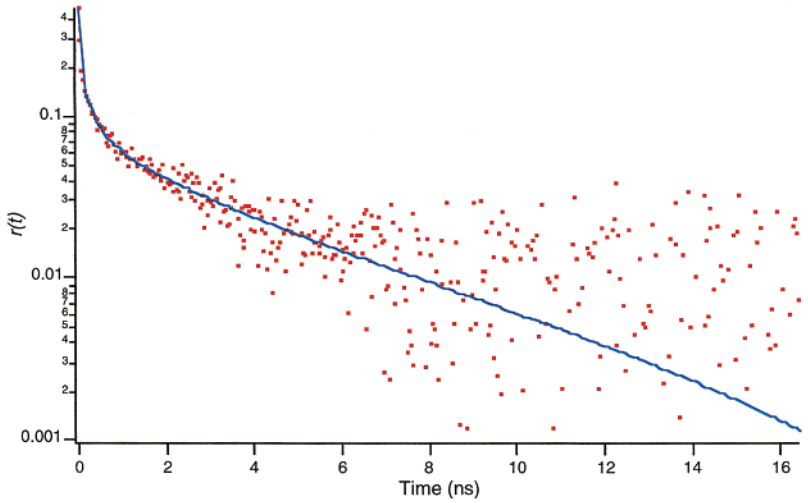

Figure 5. Fluorescence anisotropy decay $r(t)$ for C102 in aqueous ASM solutions at 294 K. Data are represented by dots, and the solid line shows the nonlinear least-squares fit to a triexponential function.

TABLE 2: Parameters of Fluorescence Anisotropy Decay of C102 in ASM/Water, PEG/Water, and Water Control Solutions

C102 solution	α_{r1}	τ_{r1} (ps)	α_{r2}	τ_{r2} (ps)	α_{r3}	τ_{r3} (ps)
ASM/water	0.66	46 ± 25^a	0.2	416 ± 25^a	0.14	4090 ± 100^a
PEG/water	1	62 ± 3^b				
water	1	68 ± 3^b				

[a] From TCSPC; time spacing: 36.4 ps/point; fluorescence upconversion data provide $\tau_{r1} = 68 \pm 3$ ps. [b] From fluorescence upconversion; time spacing: 2.8 ps/point

different concentrations and M_w values of PEG in water. The C102 fluorescence anisotropy experiments in the same concentrated aqueous PEG solutions show dynamics that are well fit to either biexponential or single exponential plus Kohlrausch models with equivalent statistical estimates of fit quality.

The friction measured by fluorescence probing of concentrated aqueous PEG solutions using the C102 probe leads to dynamics that often cannot be fit by sums of exponential functions. We consider whether these results relate to the fluorescence probing of the dilute ASM solutions. Comparing the dynamics for ASM solutions with those for PEG, we must bear in mind that three $M_w = 5000$ g mol^{-1} PEG chains are covalently tethered to the hydrophobic core of the ASM. Though ASMs were used at a concentration of about 10^{-4} M, the effective local concentration of aqueous PEG is much higher because of the tripod structure. Even though pure aqueous PEG solutions do not aggregate at low concentrations,[42,43] we cannot be certain whether the three-way tether of PEG ($M_w = 5000$ g mol^{-1}) tails of the ASM leads to homogeneous coverage with extended PEG chains or three distinct regions of PEG chains. If the former description applies, then the dynamical behavior could be similar to PEG with $M_w = 15\,000$ g mol^{-1}.

Analysis of the fluorescence anisotropy data for the C102 probe embedded in the ASM yields nearly identical results for two models. The sum of three exponential terms or the sum of single exponential plus Kohlrausch functions (eq 5) gives statistically identical fits. The origin of the shortest lifetime is not ambiguous: because we independently measured the reorientation time constant of C102 in water and dilute PEG 5000 solutions (with a time constant of 68 ps), the fastest lifetime was assigned to C102 that was released from the ASM carrier. Even 5 wt % solutions of aqueous PEG show C102 reorientation dynamics that are substantially slowed compared with those of water solutions. The dynamics of the C102 drug model in the ASM can be well described by the Kohlrausch function, with very strongly nonexponential character ($\beta = 0.485$), or equally well by a biexponential relaxation with time constants of 442 ps and 4.39 ns. In either case, the fit functions represent a broad distribution of time constants arising from a large number of possible orientations of the chromophore within the ASM.

TDFSS dynamics for C102 encapsulated within the ASM also show a complex relaxation that can be well fit to two models. For the stretched exponential solvent/polymer reorganization dynamics, the Kohlrausch parameters are $\tau_{solv} = 1.44$ ns and $\beta = 0.72$, which are substantially less extreme than those for the anisotropy. However, the triexponential model gives the best fit with the parameters shown in Table 2.

Using the multiexponential model, the reorientation time constants for PEG solutions ($M_w = 4600$ g mol^{-1}, concentrations = 10−50 wt %)[39] were found to be similar to the ones determined for the ASM (400 and 4100 ps). Thus, it is possible that a portion of the slower dynamics arises not only from C102 in the hydrophobic core of the ASM but perhaps also from C102 in the outer aqueous PEG part of the ASM.

Pertinent information about the local environments for small hydrophobic molecules encapsulated in ASMs has been obtained. Several questions remain about the probe mobility and specific location within the ASM host molecules. It is not yet clear whether the guest molecule (i.e., C102) resides predominantly in the alkyl-based lipophilic core, the PEG-based hydrophilic shell, or the core−shell interface. The C102 drug model is obviously labile, or it would not be released from the ASM. As drug delivery agents, ASMs must (and do) eventually release the encapsulated molecules. It is anticipated that pinpointing the primary location of the drug molecule will best enable control of the drug release rate. This issue will be addressed using single-molecule picosecond time-resolved fluorescence correlation spectroscopy.

Conclusions

Steady-state and time-resolved fluorescence spectroscopy revealed that solvent reorganization and diffusive reorientation of the C102 solvatochromic fluorescent probe occur on similar time scales within the interior environment of the ASM. Fluorescence methods were used to probe the local fluctuations and reorganization phenomena within polymer-based drug carriers such as the ASMs discussed here. In particular, the ASM

host encapsulates C102 guest molecules in a variety of nanoenvironments, with approximately 10% of the probe molecules experiencing substantially increased local friction. On the basis of prior drug-release data,[2] friction induced by the hydrophobic core controls the slowed release of C102 from the ASM. The information presented in this paper guides us in further exploring the mechanism of encapsulation of model drug molecules within potential polymeric drug carriers.

Acknowledgment. We thank Professor D. Talaga and Y. Issa for the use of their Igor-based iterative deconvolution software and Professor M. Maroncelli for the use of the stshany2 Fortran program for the analysis of time-dependent fluorescence Stokes shifts. We thank B. Lee, E. Diken, and Dr. P. Wiewior for sharing their data on aqueous PEG prior to publication. We thank Professors J. Völker and K. J. Breslauer for their help with the steady-state fluorescence measurements. L.F. and K.E.U. acknowledge support from the National Science Foundation (BES-9983272 to K. E. U).

References and Notes

(1) Liu, H.; Jiang, A.; Guo, J.; Uhrich, K. E. *J. Polym. Sci., Part A: Polym. Chem.* **1999**, *37*, 703.

(2) Liu, H.; Farrell, S.; Uhrich, K. *J. Controlled Release* **2000**, *68*, 167.

(3) Webber, S. E. *J. Phys. Chem. B* **1998**, *102*, 2618.

(4) Attwood, D.; Florence, A. T. *Surfactant Systems: Their Chemistry, Pharmacy, and Biology*; Chapman and Hall: London, 1983; p 293 ff.

(5) Hurter, P. N.; Alexandridis, P.; Hatton, T. A. *Solubilization in Surfactant Aggregates*; Marcel Dekker: New York, 1995; p 191 ff.

(6) Torchilin, V. P. *J. Controlled Release* **2001**, *73*, 137.

(7) Schmalenberg, K. E.; Frauchiger, L.; Nikkhouy-Albers, L.; Uhrich, K. E. *Biomacromolecules* **2001**, *3*, 851.

(8) Albers, L.; Uhrich, K. E. Middle Atlantic Regional American Chemical Society Meeting, Madison, NJ, May 1999.

(9) Elworthy, P. H.; Florence, A. T.; Macfarlane, C. B. *Solubilization by Surface Active Agents*; Chapman and Hall: London, 1968.

(10) Barbara, P. F.; Jarzeba, W. *Adv. Photochem.* **1990**, *15*, 1.

(11) Maroncelli, M. *J. Mol. Liq.* **1993**, *57*, 1.

(12) Vajda, S.; Jimenez, R.; Rosenthal, S. J.; Fidler, V.; Fleming, G. R.; Castner, E. W., Jr. *J. Chem. Soc., Faraday Trans.* **1995**, *91*, 867.

(13) Shirota, H.; Pal, H.; Tominaga, K.; Yoshihara, K. *J. Phys. Chem. A* **1998**, *102*, 3089.

(14) Lien, E. J. In *Encyclopedia of Pharmaceutical Technology*; Swarbrick, J., Boylan, J. C., Ed.; Marcel Dekker: New York, 1995; Vol 11, p 293 ff.

(15) Hagan, S. A.; Coombes, G. A.; Garnett, M. C.; Dunn, S. E.; Davies, M. C.; Illum, L.; Davis, S. S.; Harding, S. E.; Purkiss, S.; Gellert, P. R. *Langmuir* **1996**, *12*, 2153.

(16) Shirota, H.; Castner, E. W., Jr. *J. Chem. Phys.* **2000**, *112*, 2367.

(17) Castner, E. W., Jr.; Kennedy, D.; Cave, R. *J. Phys. Chem. A* **2000**, *104*, 2869.

(18) English, C. S.; Das, K.; Ashby, K. D.; Park, J.; Petrich, J. W.; Castner, E. W., Jr. *J. Am. Chem. Soc.* **1997**, *119*, 11585.

(19) Sarkar, N.; Datta, A.; Das, S.; Bhattacharyya, K. *J. Phys. Chem.* **1996**, *100*, 15483.

(20) Sarkar, N.; Das, K.; Datta, A.; Das, L.; Bhattacharyya, K. *J. Phys. Chem.* **1996**, *100*, 10523.

(21) Jimenez, R.; Fleming, G. R.; Kumar, P. V.; Maroncelli, M. *Nature (London)* **1994**, *369*, 471.

(22) Pant, D.; Levinger, N. E. *J. Phys. Chem. B* **1999**, *103*, 7846.

(23) Riter, R. E.; Undiks, E. P.; Kimmel, J. R.; Levinger, N. E. *J. Phys. Chem. B* **1998**, *102*, 7931.

(24) Maroncelli, M.; Fleming, G. R. *J. Chem. Phys.* **1987**, *86*, 6221.

(25) Horng, M. L.; Gardecki, J. A.; Papazyan, A.; Maroncelli, M. *J. Phys. Chem.* **1995**, *99*, 17311.

(26) Castner, E. W.; Chang, Y. J.; Chu, Y. C.; Walrafen, G. E. *J. Chem. Phys.* **1995**, *102*, 653.

(27) Zhang, J.; Bright, F. V. *J. Phys. Chem.* **1991**, *95*, 7900.

(28) Shirota, H.; Horie, K. *J. Phys. Chem. B* **1999**, *103*, 1437.

(29) Pierce, D. W.; Boxer, S. G. *J. Phys. Chem.* **1992**, *96*, 5560.

(30) Baskhin, J. S.; McLendon, G.; Mukamel, S.; Marohn, J. *J. Phys. Chem.* **1990**, *94*, 4757.

(31) Kovalenko, S. A.; Ruthmann, J.; Ernsting, N. P. *Chem. Phys. Lett.* **1997**, *271*, 40.

(32) Smith, G. D.; Borodin, O.; Bedrov, D.; Paul, W.; Qiu, X. H.; Ediger, M. D. *Macromolecules* **2001**, *34*, 5192.

(33) Tokmakoff, A.; Zimdars, D.; Urdahl, R. S.; Francis, R. S.; Kwok, A. S.; Fayer, M. D. *J. Phys. Chem.* **1995**, *99*, 13310.

(34) Borodin, O.; Bedrov, D.; Smith, G. D. *Macromolecules* **2001**, *34*, 5687.

(35) Adachi, K.; Saiz, E.; Riande, E. *Phys. Chem. Chem. Phys* **2002**, *4*, 635.

(36) Bordi, F.; Cametti, C.; Paradossi, G. *Biopolymers* **1995**, *36*, 539.

(37) Ngai, K. L. *Adv. Colloid Interface Sci.* **1996**, *64*, 1.

(38) Nystrom, B.; Walderhaug, H.; Hansen, F. K. *J. Phys. Chem.* **1993**, *97*, 7743.

(39) Lee, B. J.; Diken, E. G.; Wiewior, P. W.; Castner, E. W., Jr. To be submitted for publication.

(40) Nagarajan, V.; Brearley, A. M.; Kang, T. J.; Barbara, P. F. *J. Chem. Phys.* **1987**, *86*, 3183.

(41) Gardecki, J. A.; Maroncelli, M. *J. Phys. Chem. A* **1999**, *103*, 1187.

(42) Devanand, K.; Selser, J. C. *Nature (London)* **1990**, *343*, 6260.

(43) Kinugase, S.; Nakahara, H.; Fudagawa, N.; Koga, Y. *Macromolecules* **1994**, *27*, 6889.